JACS
JOURNAL OF THE AMERICAN CHEMICAL SOCIETY

COMMUNICATION

pubs.acs.org/JACS

Electrical Switching between Vesicles and Micelles via Redox-Responsive Self-Assembly of Amphiphilic Rod−Coils

Hoon Kim, Sang-Mi Jeong, and Ji-Woong Park*

Department of Materials Science and Engineering, Gwangju Institute of Science and Technology, 261 Cheomdan-gwagiro, Buk-gu, Gwangju 500-712, Korea

Supporting Information

ABSTRACT: An aqueous vesicular system that is switchable by electric potential without addition of any chemical redox agents into the solution is demonstrated using redox-responsive self-assembly of an amphiphilic rod−coil molecule consisting of a tetraaniline and a poly(ethylene glycol) block. The vesicle membrane is split by an oxidizing voltage into smaller pucklike micelles that can reassemble to form vesicles upon exposure to a reducing voltage. The switching mechanism is explained by the packing behavior of the tetraaniline units constituting the membrane core, which depends on their oxidation states.

Polymeric vesicles are usually obtained via self-assembly of amphiphilic block copolymers in solution. They possess greater stability than liposomes based on small-molecule lipids.[1,2] An important characteristic of polymeric vesicles is their switching behavior, which stems from the ability of their constituent polymer chains to change their conformation and assembly behaviors in response to external stimuli such as pH, temperature, solvent type, or concentration.[3−8] In this regard, the destabilization of polymeric vesicles via a redox reaction is of great interest because it may be useful in drug delivery in the oxidative environment of extracellular fluids.[9−12] Other applications in biosensing, biodetection, and microfluidics have been suggested.[10]

The redox-responsive disruption or reorganization of polymeric vesicles is caused by either a change in polarity of the constituting block[10,13] or cleavage of the chemical or physical bonds between hydrophobic and hydrophilic blocks.[11,14−17] In most polymeric vesicle systems reported to date, however, chemical additives must be used to induce the redox processes.[9] For some vesicle applications, it may be desirable to have a system whose structure can be switched by applying only an electrical potential without addition of chemical agents to the solution.

A vesicle system responsive to applied electric potentials was recently demonstrated with a supramolecular, amphiphilic block copolymer that formed via host−guest complexation between the end groups of a hydrophilic and hydrophobic homopolymer pair.[16] The vesicles were disrupted by scission of block copolymer amphiphiles into two homopolymers by an applied oxidative voltage. This method, however, can cause hydrophobic polymer chains to be exposed to an aqueous environment, which may lead to the formation of insoluble aggregates. An alternative way to disrupt vesicles and release their encapsulated molecules that does not completely dissociate the vesicles into their constituent molecular species is to simply rupture the membrane walls of the vesicles. Here we present such a new type of switchable vesicular system, in which the vesicle membrane is split by an oxidizing voltage into smaller micellar objects that can reassemble to form vesicles upon exposure to a reducing voltage.

We derived the voltage-responsive switching property of the vesicle utilizing the redox-responsive self-assembly characteristics of an amphiphile with a rod−coil architecture (Figure 1). The study was based on our previous findings on the morphology of lamellar crystals formed by a series of alkyltetraanilines,[18] which showed that the tetraaniline (TA) block packs more compactly in the emeraldine base (EB) state than in the leucoemeraldine base (LEB) state because of amine−imine hydrogen bonding that occurs only in the EB form (Figure S1 in the Supporting Information). The different packing densities of TA blocks in the two oxidation states resulted in different layer periodicities for the multilayered lamellar crystals of alkyl-TAs because of the different degrees of tilt angle between the TA and alkyl molecular axes.

It was anticipated that the redox-responsive packing of oligoanilines would also occur in the membranes of vesicles obtained from the oligoaniline rod−coil system with amphiphilic architecture. A rod−coil molecule (TAPEG) was synthesized by amidation of a TA block with poly(ethylene glycol) (PEG, $M_n \approx$ 550 Da) monocarboxylic acid (Figure 1a and Figure S2). Once TAPEG forms vesicles, as the packing of the TA moieties constituting the membrane core becomes more compact in response to an applied electric potential, the membrane wall should contract laterally, resulting in rupture (Figure 1b). The resultant pieces of membranes would be pucklike micelles[19−22] known for rod−coil amphiphiles. Because they are still enclosed by hydrophilic PEG chains, they should be dispersed well in aqueous solutions. The pucklike micelles would reassemble to vesicles whenever the process is reversed by a potential of opposite sign.

We examined first the redox properties and aggregation behavior of TAPEG in different oxidation states in aqueous solutions. The LEB form of TAPEG (TAPEG-LEB) could be dissolved at a concentration below 0.05 wt % and was readily converted to the EB form (TAPEG-EB) by application of an electrical potential in the presence of 0.05 M NaCl as an electrolyte, as demonstrated by cyclic voltametry (CV) data (Figure 2a) and UV−vis spectra (Figure 2b). The entire sample in an electrochemical cell could be oxidized or reduced by stirring for a sufficient period of time under the corresponding static potential (Figure S3). At 0.2 V, the LEB

Received: January 12, 2011
Published: March 18, 2011

dx.doi.org/10.1021/ja200297j | J. Am. Chem. Soc. 2011, 133, 5206–5209

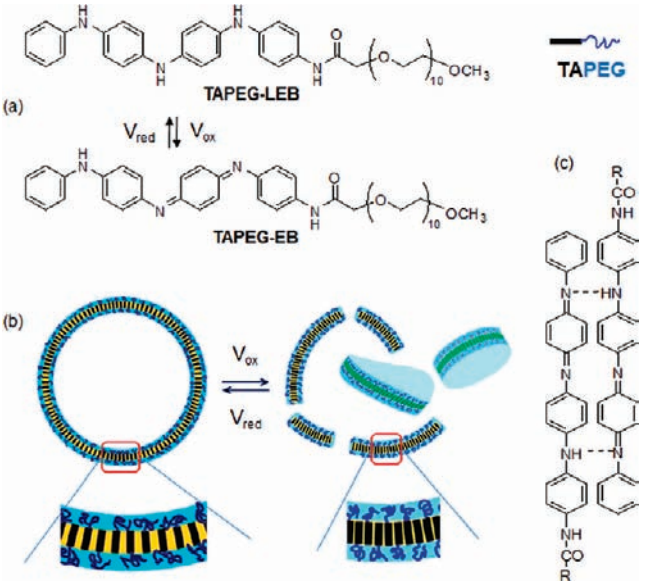

Figure 1. Voltage-responsive TAPEG rod−coils in aqueous solution. (a) Chemical structures of TAPEG in the LEB and EB oxidation states. (b) Schematic representation of redox switching between vesicles and pucklike micelles of rod−coils that would be induced by the change in packing density in the membrane core. The membrane shrinks laterally upon oxidation of TA units from the LEB state to the EB state, resulting in rupture of the vesicles. It should be noted that the cartoon represents only a cross section of a two-dimensional membrane layer to emphasize the difference in intermolecular packing density. (c) Amine−imine intermolecular hydrogen bonding in the EB form of TAPEG.

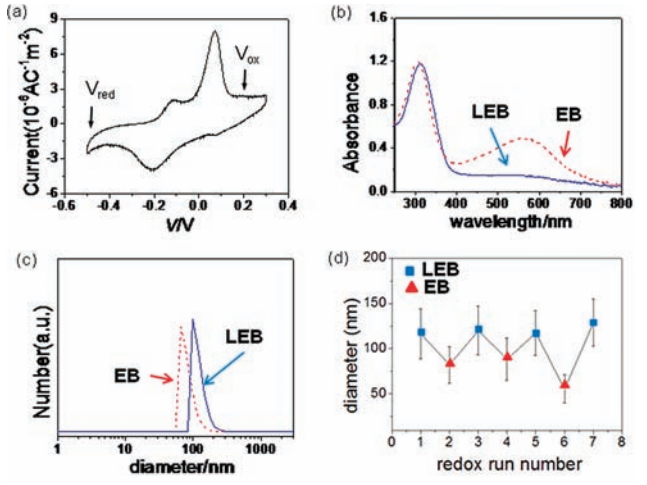

Figure 2. Electrical switching of the aggregation behavior of TAPEG rod−coils. (a) CV curve for TAPEG at a concentration of 0.05 mg/mL in an aqueous 0.05 M NaCl solution. CV was scanned over the range from −0.5 to 0.3 V (vs Ag/Ag$^+$). V_{ox} (0.2 V) and V_{red} (−0.5 V) are the static potentials applied to the TAPEG solutions to obtain the EB and LEB forms, respectively. (b) In situ UV−vis spectra of the TAPEG solutions at 0.2 V (EB state) and −0.5 V (LEB state). (c) Number distributions of DLS particle sizes for TAPEG-LEB and -EB. (d) Peak DLS particle diameters recorded at 0.2 and −0.5 V in multiple consecutive redox runs.

molecules were converted into the EB form, and the reverse process occurred at −0.5 V.

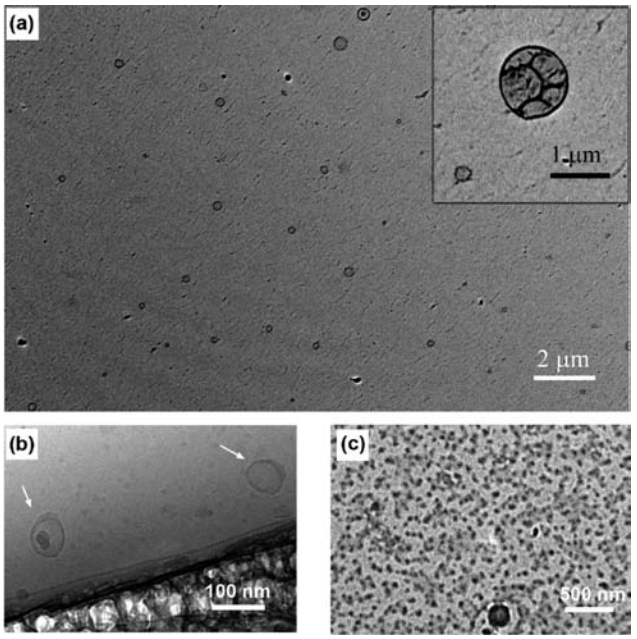

Figure 3. TEM images of vesicles and micelles. (a) Images of the vesicular objects of various sizes captured on a carbon support film. The solution reduced at −0.5 V was cast onto a carbon-coated copper grid and rapidly evaporated. The inset shows a magnified image of a giant collapsed vesicle found on the same TEM grid. (b) CryoTEM image of the vesicle. (c) Micellar objects prepared from the solution oxidized at 0.2 V. Images (a) and (c) were obtained from the samples corresponding to redox runs 5 and 6, respectively, in Figure 2d.

Dynamic light scattering (DLS) data (Figure 2c,d) for aqueous 0.001−0.05 wt % TAPEG solutions in the presence of 0.05 M NaCl showed that the molecules self-assembled into different types of nanoscale aggregates in the LEB and EB states that were interchangeable by applying a redox potential. The peak DLS diameters varied over the ranges of 110−130 nm for the LEB state and 60−90 nm for the EB state as the applied potential was switched between −0.5 and 0.2 V, respectively. The system could be repeatedly switched between states. The reversible change in DLS particle size suggests that amphiphilic rod−coils self-assemble into different morphologies at the two applied potentials.

To identify the structures of the objects formed in the two oxidation states, we obtained transmission electron microscopy (TEM) images for the samples prepared directly from the TAPEG solutions oxidized or reduced by voltage (Figure 3). TAPEG-LEB exhibited a strong tendency to form vesicular objects. In most samples prepared by evaporation of solvent (water) on carbon-coated copper TEM grids, objects with a hollow vesicular morphology and various sizes from ∼100 nm to a few micrometers appeared (Figure 3a and Figure S4). Because the TEM images of the smaller vesicles in the solution-cast specimens were often obscured by electron beam damage, the presence of small vesicles was further confirmed by cryogenic TEM (cryo-TEM) for an aqueous solution (Figure 3b). Because the size of the particles in the LEB solutions appeared to be at most several hundred nanometers on the basis of the DLS data, the giant vesicles captured on the substrate surface were most likely to be generated during evaporation of the solvent (water). Increasing the solution concentration above 0.05% caused turbidity, indicative of the formation of larger aggregates at higher concentrations. In contrast to the LEB state, the EB state

dx.doi.org/10.1021/ja200297j |J. Am. Chem. Soc. 2011, 133, 5206–5209

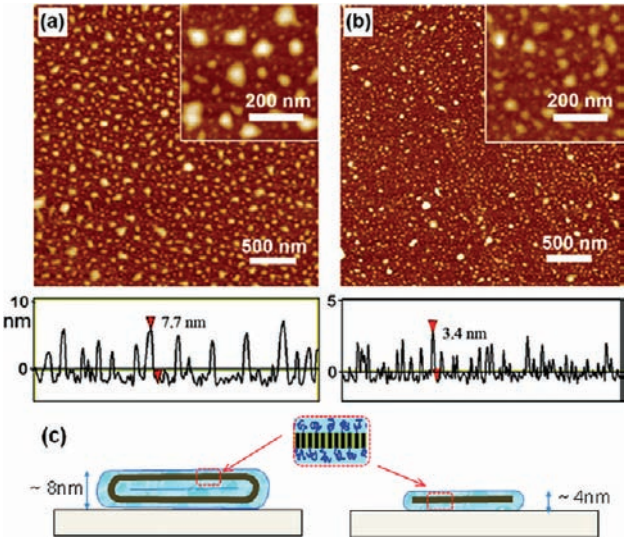

Figure 4. Vesicles and puck micelles captured on the substrate surface. (a, b) Height-contrast AFM images of the (a) LEB and (b) EB states of TAPEG. The corresponding cross-sectional height profile is given underneath each image. Images (a) and (b) were obtained from the samples corresponding to redox runs 3 and 4, respectively, in Figure 2d. A droplet of the solution from the electrochemical cell was cast onto wafer plates and then blotted immediately with filter paper and dried under atmospheric conditions. (c) Schematic model of a dry vesicle and a pucklike micelle collapsed on the surface.

of TAPEG samples on the TEM grids yielded nonhollow particulate objects (Figure 3c). Dendritic aggregates were sometimes observed on the substrate surface (Figure S5), likely resulting from either aggregation of the particulate objects or crystallization of the PEG chains on the substrate surface. Overall, the TEM images and DLS data together indicate that TAPEG molecules in the LEB state form vesicles that are transformed to smaller micelles upon oxidation to the EB state.

We used atomic force microscopy (AFM) to further understand the molecular arrangements in the two oxidation states of TAPEG in solution. A droplet of the solution in the electrochemical cell was cast onto air-plasma-treated silicon wafer plates and then blotted immediately with filter paper and dried. Rapid solvent (water) evaporation from the residual solution on the hydrophilic substrate surface prevented the formation of macroscopic aggregates and instead enabled more individual objects to be captured. Indeed, the AFM images (Figures 4) in both oxidation states showed objects distributed uniformly over the substrate surface with a lateral dimension close to the range of the corresponding DLS data of Figure 2.

The objects captured on the AFM specimens were nonspherical: the thickness of the objects appeared to be much smaller than their width or diameter and had maximum values of ~8 nm for the LEB state (Figure 4a) and ~4 nm for the EB state (Figure 4b). The LEB form was, on average, twice as thick as the EB form. This result can be explained by considering the packing model of the rod−coil amphiphiles in the vesicles and pucklike micelles, as suggested in Figure 4c. TA blocks (having a theoretical length of 2.0 nm) pack in an interdigitated, smectic manner to form a crystalline hydrophobic core, and the PEG blocks emanating from the TA block constitute the hydrophilic shell on both sides of the core. Because the flexible PEG moiety has a weight fraction similar to the remaining part of TAPEG, the

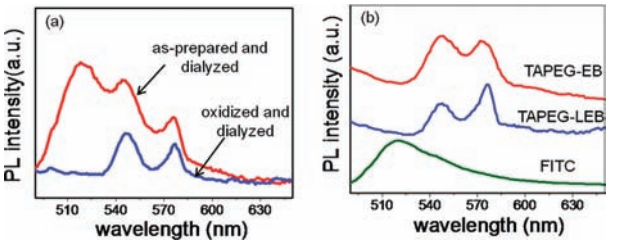

Figure 5. Probe loading and release by the voltage-responsive vesicles. (a) PL spectra of the as-prepared mixture of TAPEG-LEB and FITC (red) and the corresponding mixture after oxidation at 0.2 V (blue). Both solutions were dialyzed before the PL measurement (λ_{ex} = 460 nm). (b) Control PL spectra of pure TAPEG-EB (red), TAPEG-LEB (blue), and FITC (green) in aqueous solution.

resultant vesicle membrane should be ~4 nm thick. This is consistent with the thickness of the vesicle membrane estimated from the cryo-TEM image (Figure 3b). Upon evaporation of the solvent, the hollow vesicles in the LEB state collapse onto the substrate surface to form 8 nm thick double-layered objects, whereas in the EB state, they form 4 nm thick single-layered plates. When the vesicles are dried, the orientation of the molecular axis (director) with respect to the substrate plane can be altered, causing the observed thickness of the objects on the surface to be smaller than the maximum values for the vertical director orientation.

On the basis of the data shown in Figures 2−4 and the crystallization behaviors of alkyl-TA rod−coils observed in our previous study,[18] we postulate that the switching between vesicles and puck micelles occurs via the mechanism represented in Figure 1b. The change in hydrophilicity of the TA units by chemical doping cannot be considered as a switching mechanism because the UV absorption spectra in Figure 2b indicate that the oxidation from the LEB form to the EB form does not involve chemical doping. In a control experiment, the signals for nanoscale aggregates disappeared from the DLS data when the pH of the solution was lowered below 4, indicating that TAPEG molecules become completely soluble because the oxidation of TA units involves chemical doping with acids.

In contrast, the structural change that occurs by the mechanism suggested in Figure 1 is rapid and reversible because the configurations of intermolecular packing in the vesicle membrane and the puck micelles are almost identical. Oxidation-induced compact packing of the TA blocks with the conformation of the PEG chains left unchanged leads to lateral shrinkage in the hydrophobic core of the vesicular membrane and eventually to breakage of their hollow structures into multiple pucklike micelles. The discrete micelles cannot recombine to yield smaller vesicles because of the rod−coil packing frustration that comes from disparate interfacial areas per chain at the rod−coil junction in the EB state.[19,21,22] Upon reduction to the LEB state, the micelles become interconnected to form a continuous vesicle membrane, which is thermodynamically more stable.

To demonstrate the potential of electrically switchable vesicles in molecular delivery, we investigated their encapsulation and release behavior toward a photoluminescence (PL) probe, fluorescein isothiocyanate (FITC) (Figure 5). TAPEG-LEB and NaCl were first mixed with a solution of FITC, and then unencapsulated FITC was removed by dialysis. The PL spectrum of the FITC-loaded vesicle solution was recorded, after which the solution was oxidized at 0.2 V and then dialyzed. Because the TA

moieties also exhibited characteristic PL spectra in both the LEB and EB forms (Figure 5b), the presence of TAPEG and FITC in the solutions could be easily detected by this experiment. As a result, the FITCs encapsulated by the vesicles in the LEB state were retained during dialysis, whereas after oxidation to the EB state, the FITCs were removed completely by dialysis. The TAPEG molecules remained during dialysis in both oxidation states because they exist in the form of vesicles in the LEB state and micelles in the EB state.

In summary, we have demonstrated a new electrically switchable vesicular system based on redox-responsive self-assembly of amphiphilic rod−coil molecules consisting of an oligoaniline and a PEG block. The vesicles are ruptured to form pucklike micelles by an oxidizing voltage, and the micelles regenerate vesicles upon application of a reducing voltage. The mechanism of vesicle rupture was explained by lateral shrinkage of the vesicle membrane caused by the change in the density of the parallel packing of the rodlike oligoaniline moieties constituting the hydrophobic core. The assembly behavior was reversibly controlled without altering the chemical composition, concentration, volume, or temperature. The electrically switchable packing behaviors of redox-active rod−coil amphiphiles may be promising for creation of new vesicle systems for molecular delivery in biomedical or microfluidic devices.

■ ASSOCIATED CONTENT

Supporting Information. Experimental details, SAXS/WAXS graphs of dodecyltetraaniline (TADD-EB and -LEB) crystals, ^{1}H NMR spectra of TAPEG-LEB and -EB, UV spectra of TAPEG with time during oxidation, and more TEM images of the vesicles. This material is available free of charge via the Internet at http://pubs.acs.org.

■ AUTHOR INFORMATION

Corresponding Author
jiwoong@gist.ac.kr

■ ACKNOWLEDGMENT

This research was supported by the Basic Science Research Program (2010-0000282) through the National Research Foundation of Korea (NRF), funded by the Ministry of Education, Science, and Technology of Korea, and by the Program for Integrated Molecular Systems (PIMS) at GIST. The authors thank Prof. T. Kawai and Mr. A. Tanaka in the Graduate School of Materials Science at Nara Institute of Science and Technology, Japan, for helping us to obtain the cryo-TEM image of vesicles.

■ REFERENCES

(1) Discher, B. M.; Won, Y.-Y.; Ege, D. S.; Lee, J. C.-M.; Bates, F. S.; Discher, D. E.; Hammer, D. A. *Science* **1999**, *284*, 1143–1146.
(2) Discher, D. E.; Eisenberg, A. *Science* **2002**, *297*, 967–973.
(3) Li, Y.; Smith, A. E.; Lokitz, B. S.; McCormick, C. L. *Macromolecules* **2007**, *40*, 8524–8526.
(4) Hu, Z.; Jonas, A. M.; Varshney, S. K.; Gohy, J.-F. *J. Am. Chem. Soc.* **2005**, *127*, 6526–6527.
(5) Chiu, H.-C.; Lin, Y.-W.; Huang, Y.-F.; Chuang, C.-K.; Chern, C.-S. *Angew. Chem., Int. Ed.* **2008**, *47*, 1875–1878.
(6) Broz, P.; Driamov, S.; Ziegler, J.; Ben-Haim, N.; Marsch, S.; Meier, W.; Hunziker, P. *Nano Lett.* **2006**, *6*, 2349–2353.
(7) Vriezema, D. M.; Comellas Aragones, M.; Elemans, J. A. A. W.; Cornelissen, J. J. L. M.; Rowan, A. E.; Nolte, R. J. M. *Chem. Rev.* **2005**, *105*, 1445–1490.
(8) Koh, H. D.; Park, J. W.; Rahman, M. S.; Changez, M.; Lee, J. S. *Chem. Commun.* **2009**, 4824–4826.
(9) Du, J. Z.; O'Reilly, R. K. *Soft Matter* **2009**, *5*, 3544–3561.
(10) Napoli, A.; Valentini, M.; Tirelli, N.; Muller, M.; Hubbell, J. A. *Nat. Mater.* **2004**, *3*, 183–189.
(11) Ma, N.; Li, Y.; Xu, H. P.; Wang, Z. Q.; Zhang, X. *J. Am. Chem. Soc.* **2010**, *132*, 442–443.
(12) Cerritelli, S.; Velluto, D.; Hubbell, J. A. *Biomacromolecules* **2007**, *8*, 1966–1972.
(13) Power-Billard, K. N.; Spontak, R. J.; Manners, I. *Angew. Chem., Int. Ed.* **2004**, *43*, 1260–1264.
(14) Wang, C.; Guo, Y. S.; Wang, Y. P.; Xu, H. P.; Zhang, X. *Chem. Commun.* **2009**, 5380–5382.
(15) Dong, W. F.; Kishimura, A.; Anraku, Y.; Chuanoi, S.; Kataoka, K. *J. Am. Chem. Soc.* **2009**, *131*, 3804–3805.
(16) Yan, Q. A.; Yuan, J. Y.; Cai, Z. N.; Xin, Y.; Kang, Y.; Yin, Y. W. *J. Am. Chem. Soc.* **2010**, *132*, 9268–9270.
(17) Plamper, F. A.; Murtomaki, L.; Walther, A.; Kontturi, K.; Tenhu, H. *Macromolecules* **2009**, *42*, 7254–7257.
(18) Kim, H.; Park, J.-W. *J. Mater. Chem.* **2010**, *20*, 1186–1191.
(19) Halperin, A. *Macromolecules* **1990**, *23*, 2724–2731.
(20) Lee, M.; Cho, B.-K.; Zin, W.-C. *Chem. Rev.* **2001**, *101*, 3869–3892.
(21) Park, J. W.; Thomas, E. L. *Macromolecules* **2004**, *37*, 3532–3535.
(22) Raphael, E.; deGennes, P. G. *Physica A* **1991**, *177*, 294–300.